3.5 RECONSTRUCTION OF THE OCEANIC PRECIPITAION FROM 1948 TO THE PRESENT

Mingyue Chen[1)*], Pingping Xie[2)], John E. Janowiak[2)],
Phillip A. Arkin[3)], and Thomas M. Smith[4)]

1) RS Information System, Inc.
2) Climate Prediction Center/NCEP/NOAA
3) ESSIC, University of Maryland
4) National Climatic Data Center/NOAA

1. INTRODUCTION

In recent years, several merged analyses of global monthly precipitation have been produced and applied successfully in climate analysis and numerical model verifications (e.g. Huffman et al., 1997; Xie and Arkin, 1997). These analyses, however, cover only the most recent two decades due to their dependence on estimates from satellite observations. A precipitation analysis with extended temporal coverage is desired for many applications.

To this end, a project has been launched at the NOAA Climate Prediction Center (CPC) to construct an analysis of global monthly precipitation for a 50-year+ period from 1948 to the present. Called PREC (Precipitation REConstruction), this global analysis is composed of two parts: the land (PREC/L) and the oceanic (PREC/O) components. The land portion of this analysis is defined by optimal interpolation of gauge observations. The construction of this land analysis has been completed (Chen et al. 2002) and the data set is now available through anonymous ftp (ftp.ncep.noaa.gov).

The oceanic analysis (PREC/O) is produced by EOF reconstruction of historical gauge observations over islands and land areas. This paper describes the definition, validation and applications of the reconstructed precipitation over the global oceanic areas.

2. METHODOLOGY AND DATA

The EOF reconstruction technique of Smith et al. (1996) was used here to create analyses of monthly precipitation anomalies on a 2.5° latitude/longitude grid over the global oceanic areas (60°S-75°N) and for a time period from 1948 to the present. The EOF technique defines oceanic precipitation anomalies by projecting historical gauge observations over islands and land areas onto EOF patterns derived from satellite-based estimates for later years.

First, an EOF analysis is performed for the satellite estimates for a base period to define spatial patterns of dominant EOF modes for the target precipitation field. The time varying components for these dominant EOF modes are then computed by fitting the historical observations onto the EOF spatial functions. The reconstructed precipitation anomalies are finally defined by multiplying the EOF spatial functions with the time components for the dominant EOF modes, assuming that the EOF patterns for the target period is the same as those for the later base period.

In this study, precipitation estimates derived from the OLR-based precipitation index (OPI, Xie and Arkin 1998) were used as the satellite estimates. A 20-year period from 1979 to 1998 was selected as the base period for which the EOF patterns were defined from the OPI data. The historical gauge observations are those from the combination of two data sets: the Global Historical Climatology Network (GHCN) archived at the NOAA National Climatic Data Center (NCDC), and the Climate Anomaly Monitoring System (CAMS) data set maintained by the NOAA/CPC. These observations cover a 53-year period from 1948 to 2001. To ensure reasonable temporal stability and spatial representativeness, only the observations at stations with 10 years or longer record during the 20-year period from 1979 to 1998 and correlate with local OPI estimates better than 50% were selected as historical data.

The first 8 EOF modes were included in the reconstruction of monthly precipitation anomaly over the global oceanic areas. Previous work (Xie et al. 2002) showed that these EOF modes account for 61%, 57%, 47% and 51% of the total variance for global oceanic precipitation for the DJF, MAM, JJA, and SON periods, respectively.

3. VALIDATION

Three sets of tests were conducted to examine the accuracy of the reconstructed anomaly fields in representing large-scale precipitation variability.

3.1 Cross Validation for EOF Patterns

First, cross validation tests were conducted to examine how stable the EOF patterns are and how well they can represent the large-scale variability of oceanic precipitation. These tests are necessary because the EOF reconstruction

Corresponding author address: Mingyue Chen, RSIS/Climate Prediction Center, NOAA/NWS/NCEP/5200 Auth Road, Room 605, Camp Spring, MD 20746.

method is applied to the 1948 to 1978 time period, which is beyond the base period of 1979 – 1998 for which the EOF spatial functions are derived.

The cross validation was conducted as follows. Each time, a sub-period of 2 consecutive years was selected from the 20-year period from 1979 to 1998. EOF spatial patterns were derived using the OPI data for the remaining 18 years. These patterns were then used to define the reconstructed precipitation fields for the withdrawn 2-year period. This process was repeated for 10 times to cover the entire period of 20 years.

The reconstructed precipitation fields based on the 18-year OPI data were then compared to the withdrawn OPI estimates to examine the stability and accuracy of the reconstruction. To get insight into the performance of the reconstructed anomaly fields in representing large-scale precipitation variability, components associated with ENSO and several major circulation patterns were examined. The circulation patterns examined here include the North Atlantic Oscillation (NAO), the Pacific / North American (PNA) mode, the eastern Atlantic (EA) mode, the Western Pacific (WP) mode, and the Eastern Pacific (EP) mode (Barnston and Livezey, 1987).

The first line of Table 1 shows the comparison results for total anomaly and components associated with ENSO and major circulation patterns. It is clear that while the correlation for the total anomaly is relatively low (0.546), those for the ENSO and major climate signals are high. Together with results reported in details in Xie et al. (2002), these results show that the reconstruction is able to represent large-scale precipitation variability with reasonable accuracy over most of the tropical oceanic areas.

3.2 Cross Validation for Historical Data

The second set of tests were designed to examine the reconstruction accuracy and its dependence on the number of historical gauge observations used to define the time varying components of the reconstruction.

To do this, 10% of grid boxes with gauge observations were selected randomly as the independent gauge grid boxes. Gauge observations over the remaining 90% of the grid boxes were used to reconstruct anomalies for this 10% of grid boxes. This process was repeated 10 times so that each grid box with gauge data was withdrawn once. The reconstructed precipitation anomalies computed this way were then compared to those based on the withdrawn *gauge data* to get insight into the impact of the available historical gauge observations on the reconstruction accuracy. The results are shown in the second line of table 1.

Similar to those in the cross validation for the EOF patterns, the correlation for the total anomaly is relatively low (0.322), while those for the ENSO and major circulation patterns, ranging from 0.797 to 0.492, are reasonably high. Overall, the correlation coefficients in the cross validation for the historical data (Line 2) are not as high as those in the cross validation for the EOF patterns (Line 1). At least part of the reason for this degradation is attributed to the fact that the reconstruction is compared to the gauge observations in the cross validation for the historical data, while their count parts are OPI estimates which are less noisy than the gauge data.

Fig.1 shows the time series of 5-month running mean of the NINO3.4 SST index (top panel), and precipitation averaged over central (middle panel; 5^oS-5^oN, 160^oE-160^oW) and western Pacific (bottom panel; 5^oS-5^oN,110^oE-140^oE) as obtained from gauge observations (red) and reconstruction (green). The reconstruction exhibits close agreements with the gauge observations in large-scale temporal variation patterns. The high frequency fluctuations in the original gauge data (not shown) have been smoothed out, yielding a better agreement between the reconstruction and the gauge data. Also noticeable is a reduced magnitude in the reconstructed precipitation fields compared to that in the gauge observations. This reduction is caused by a combination of multiple factors, including the limitation of reconstruction of including only the first 8 EOF modes, and the inconsistency between gauge observations and the OPI satellite estimates.

3.3 Comparison with OPI Estimates

The last set of the validation tests is to compare the reconstruction with the OPI satellite estimates. The OPI estimates used in this study cover a 28-year period from June 1974 to December 2001, with data from March – December 1978 missing. Since the OPI estimates for the 20-year period from 1979 to 1998 are used in the definition of the reconstruction, the comparison is conducted separately for two sets of sub-periods: the dependent period extending from 1979 to 1998, and the independent periods covering from 1974 to 1978 and 1999 to 2001.

The correlation between the OPI estimates and the reconstruction (fig.2) is quite good over most of the tropical oceanic areas, with correlation higher than 0.7 over central and western tropical Pacific where precipitation variability is dominated by ENSO. The correlation is relatively low over extra-tropical oceans, indicating that the reconstruction has limited ability in retrieving precipitation variability over there.

Lines 3 and 4 of table 1 list the correlation coefficients between the reconstruction and the OPI for the dependent and independent periods, respectively. Once again, while the correlation for the total anomaly is low, the signals associated with large-scale circulation patterns are represented well in the reconstruction compared to the OPI in both the dependent and independent periods.

Although the validation tests described above are preliminary in nature, the results here show that the reconstruction using the first 8 EOF modes is able to retrieve precipitation variation associated with ENSO and major large-scale circulation patterns with reasonable accuracy. The reconstruction, however, is poor at picking up variability over extra-tropics and presents may present reduced magnitude compared to the observations.

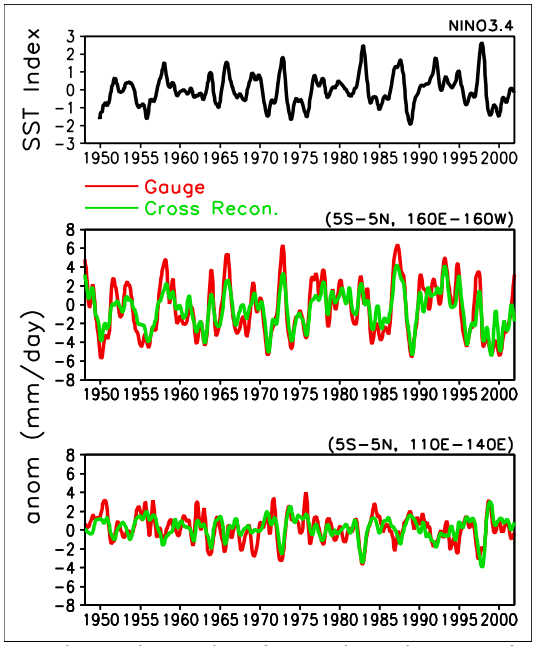

Fig. 1. Time series of 5-month-running mean for the SST index over the Nino3.4 region (the top panel, unit is ^{o}C), the precipitation anomalies averaged over the east (the middle panel) and west (the lower panel) centers of large precipitation variations related to the ENSO. The red line is for the original gauge observations and the green line is for the independent reconstruction.

4. APPLICATIONS

As part of our efforts to examine the best strategy to apply the data set, the reconstructed monthly precipitation anomaly fields were compared with those from the NCEP/NCAR reanalysis. Fig. 3 shows the time-longitude sections of SST (left; Smith, et al. 1996), and precipitation estimates obtained from the OPI (2nd from left), reconstruction (3rd from left), and the reanalysis (right) averaged over a tropical belt between 10^{o}S and 10^{o}N. The anomaly pattern associated with the evolution of ENSO was well captured by the reconstruction as evidenced by its good agreement with the OPI estimates for the period from 1974. The reanalysis, meanwhile, presents anomaly patterns with displacement in zonal direction compared to that in the OPI estimates and the reconstruction. For the period before 1974 when no satellite estimates (OPI) are available, the reconstruction exhibits variation patterns that are coherent with those of tropical SST. The anomaly patterns in the reanalysis precipitation fields, however, are less organized and weaker than those in the reconstruction.

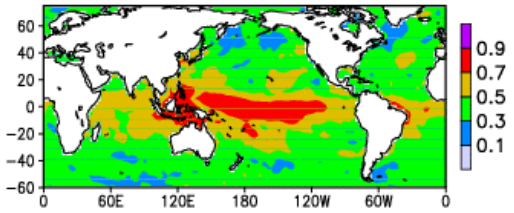

Fig. 2 The temporal correlations between the total anomalies from the PREC/O and the OPI for the dependent period.

TABLE 1. Correlations between the reconstructed precipitation anomalies and independent observations in Line 1) cross validation for EOF patterns; 2) cross validation for historical data; 3) comparison with OPI in dependent period; and 4) comparison with OPI in independent periods.

	Total	*ENSO*	*PNA*	*WP*	*EP*	*NAO*
Cross EOF	0.546	0.917	0.773	0.721	0.272	0.607
Cross Hist. Data	0.322	0.797	0.589	0.575	0.534	0.492
Dep.	0.646	0.983	0.888	0.872	0.766	0.809
Indep.	0.367	0.802	0.766	0.657	0.726	0.604

5. SUMMARY AND CONCLUSIONS

A new method is developed to define monthly precipitation anomaly over global oceans by projecting the historical gauge observations over islands and land areas onto EOF patterns derived from OPI satellite estimates for later years. A series of validation tests have been conducted and the results showed that the reconstruction is able retrieve precipitation variations associated with ENSO and major large-scale circulation patterns with reasonable accuracy. The performance, however, is poor over extra-tropical oceans and may present

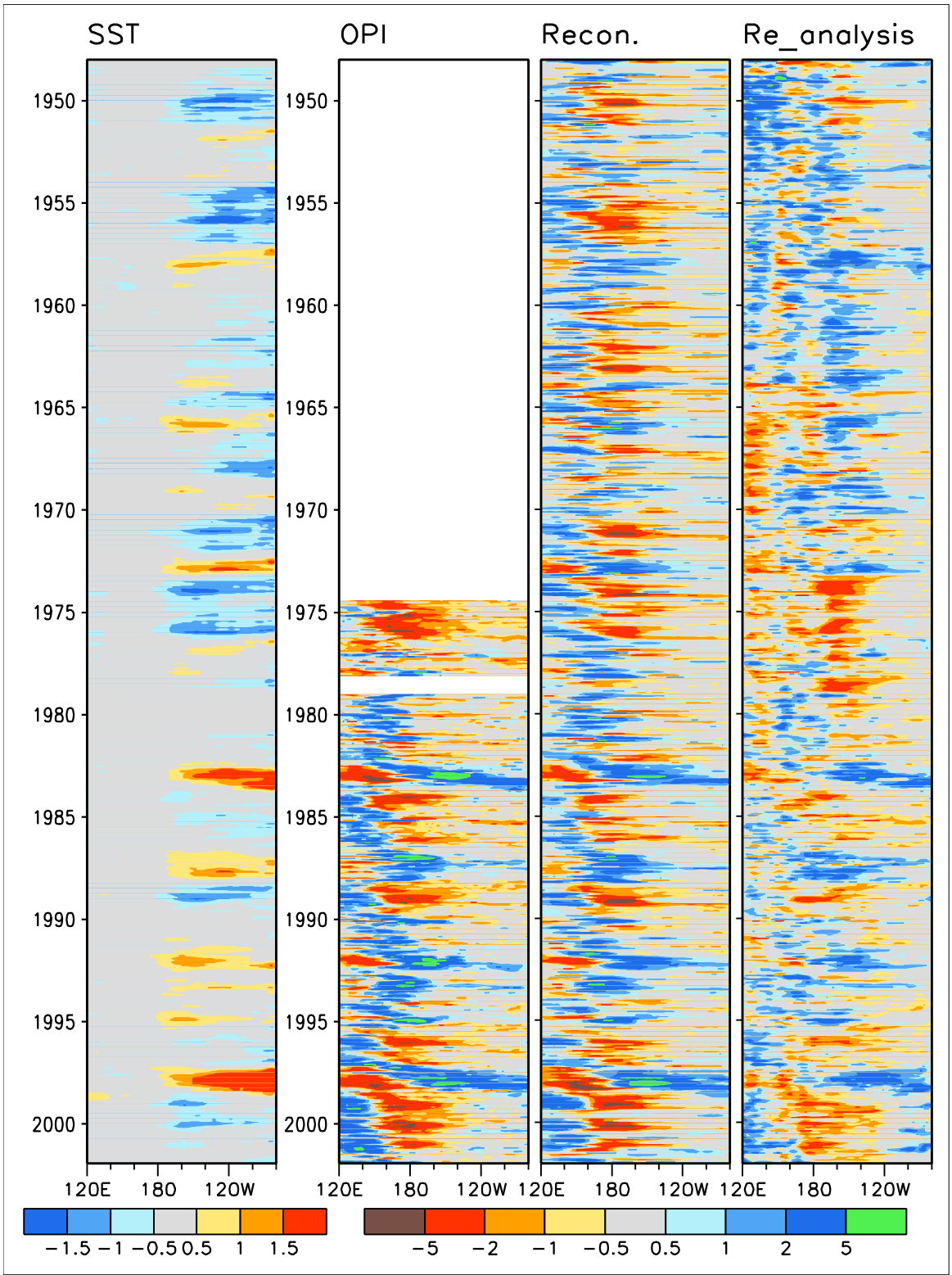

Fig. 3 Time-longitude cross-selections for the SST anomalies (^{o}C) and the precipitation anomalies (mm/day) of the PREC/O. OPI. And NCAR/NCEP Re-analysis (averaged between 10^{o}S and 10oN) for the period from 1948-2001.

reduced magnitude in the reconstructed anomaly fields.

Called PREC/O (Precipitation REConstruction over Ocean), the reconstructed precipitation anomalies are compared with the OPI estimates and with the precipitation fields produced by the NCEP/NCAR reanalysis. Preliminary results demonstrated that the reconstructed data set is potential useful in many applications.

More work is under way to improve the current version of the reconstruction and to conduct a series of verifications to gain comprehensive understanding of the performance of the reconstruction.

REFERENCES

Barnston, A. G., and R. E. Livezey, 1987: Classification, seasonality and persistence of low-frequency atmospheric circulation patterns. *Mon. Wea. Rev.*, **155**, 1083-1126.

Chen, M., P. Xie, J. E. Janowiak and P. A. Arkin, 2002: Global land precipitation: A 50-yr monthly analysis based on gauge observations. *J. Hydrometeor.*, **3**, 249-266.

Huffman, and Coauthors, 1997: The Global Precipitation Climatology Project (GPCP) combined precipitation dataset. *Bull. Amer. Meteor. Soc.*, **78**, 5-20.

Smith, T. M., R. W. Reynolds, R. E. Livezey, and D. C. Stokes, 1996: Reconstruction of historical sea surface temperature using empirical orthogonal functions. *J. Climate*, **9**, 1403-1420.

Xie, P. and P. A. Arkin, 1997: Global precipitation: A 17-year monthly analysis based on gauge observations, satellite estimates and numerical model outputs. *Bull. Amer. Meteor. Soc.*, **78**, 2539-2558.

Xie, P. and P. A. Arkin, 1998: Global monthly precipitation estimates from satellite-observed outgoing longwave radiation. *J. Climate*, **11**, 137-164.